



Original Research Article

Synthesis and Characterization of Cisplatin Magnetic Nanocomposite

Haniye Pourfaraj¹ , Somayyeh Rostamzadeh Mansour^{1*} , Mohammad Zaefizadeh² ,
Arash Vojood³

¹ Department of Chemistry, Ardabil Branch, Islamic Azad University, Ardabil, Iran

² Department of Biology, Ardabil Branch, Islamic Azad University, Ardabil, Iran

³ Young Researchers and Elite Club, Ardabil Branch, Islamic Azad University, Ardabil, Iran

ARTICLE INFORMATION

Received: 06 March 2023

Received in revised: 25 March 2023

Accepted: 01 April 2023

Available online: 03 April 2023

Checked for Plagiarism: YES

DOI: [10.48309/JMNC.2023.1.6](https://doi.org/10.48309/JMNC.2023.1.6)

KEYWORDS

Synthesis

Nanocomposite

Magnetite

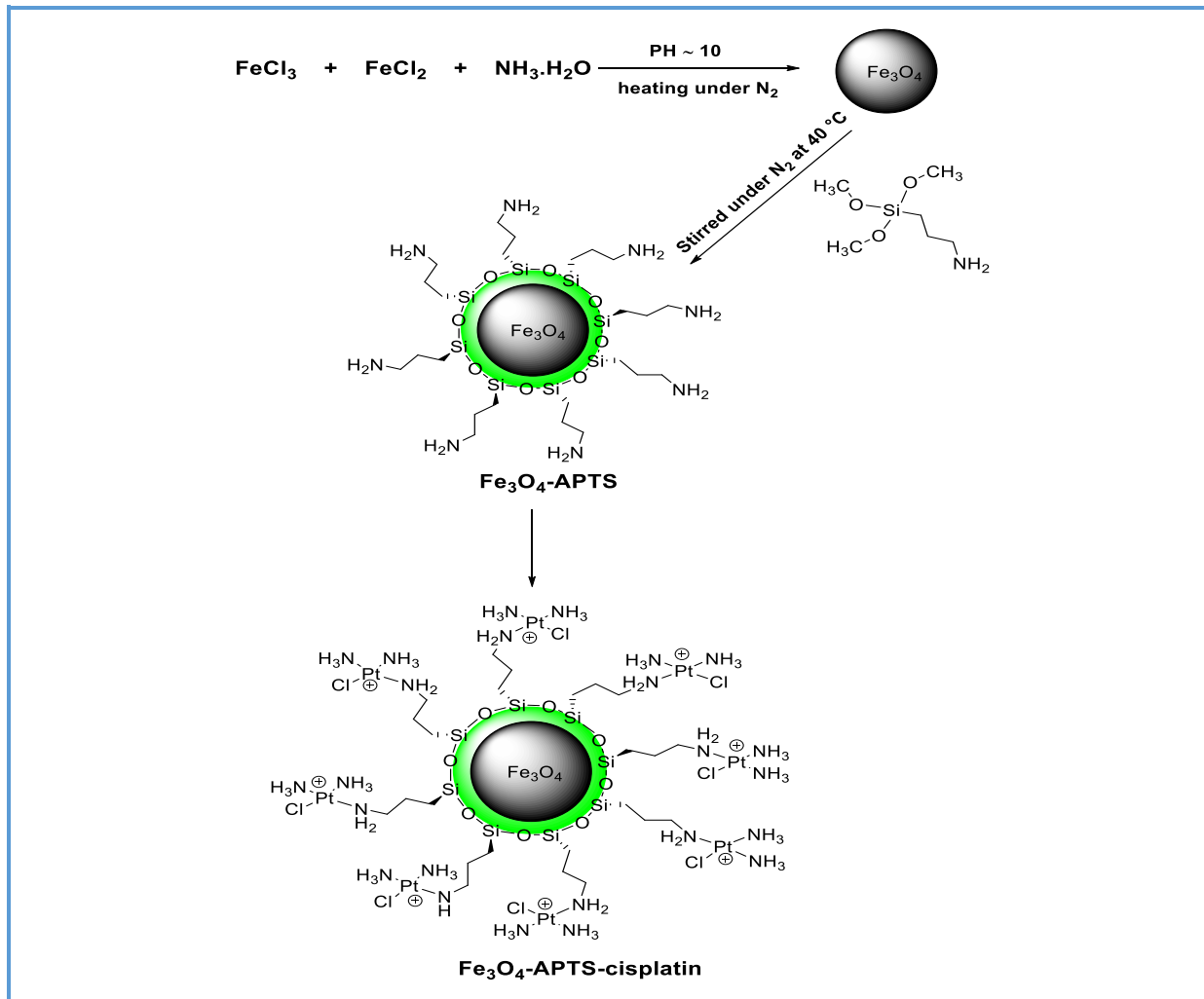
Cisplatin

Tumor

ABSTRACT

Nanotechnology is a branch of science that has opened new research horizons, particularly in the field of medicine and cancer treatment. In the present paper, magnetite nanoparticles (Fe_3O_4) were produced by co-precipitating two and three valent iron chloride salts in an alkaline medium. The surface of the nanoparticles was functionalized with (3-Aminopropyl)-trimethoxysilane (APTS), and finally, the cisplatin anticancer drug was loaded onto the modified nanoparticles. The microstructure and morphology of the nanoparticles were evaluated using X-ray diffraction (XRD), Fourier transform infrared spectroscopy (FT-IR), scanning electron microscopy (SEM), transmission electron microscopy (TEM). The magnetic properties of the material were assessed using the vibrating sample magnetometer (VSM). The results revealed that cisplatin was attached to the surface of the nanoparticles confirmed by FT-IR analysis. Magnetic properties using VSM results showed that the nanocomposite is the result of superparamagnetism. Findings showed that magnetic cisplatin nanocomposites are promising for targeted magnetic drug delivery and can be used as a targeted nanoparticle suitable for delivering anticancer drugs.

Graphical Abstract



Introduction

Nanoparticles with diameters of less than 20 to 30 nm are most commonly used in targeted drug delivery because they have fewer surface atoms, have properties such as surface tension and high solubility and are limited in size to a single crystal. The nanoparticles of larger than 30 nm are lattice-crystalline in shape and have optical and electronic properties and larger nanoparticles of 40 to 50 nm have magnetic, thermal, optical, and electronic properties. Magnetic iron nanoparticles are typical nanoparticles among other metallic nanoparticles [1, 2]. Nanoparticles have a

variety of sizes and shapes that include a variety of domains, branches, shells, tubes, emulsions, and liposomes. They can also act as a nanocarrier for cancer through encapsulation, and after targeting and releasing the drug, they do not accumulate in and decompose to the target cell. Spherical nanoparticles can carry cancer drug molecules, both hydrophobic and hydrophilic [3, 4]. Magnetic materials are substances that respond to an external field and are absorbed or repelled by it. Magnetic materials are used to develop new technologies based on metals such as iron, cobalt, nickel, or metal oxides. Magnetic materials can be applied in many devices, such as motors, sensors, and

disks. Nanoparticles have properties such as conductivity and mechanical strength. Tiny magnetic materials (magnetic nanoparticles) have different properties than other nanoparticles. The size of the smaller magnetic iron nanoparticles is about 20 nm.

Magnetic nanoparticles, which are typically Ferromagnetic and Ferrimagnetic, lose their magnetic properties at temperatures below a certain temperature. The temperature at which permanent magnets are converted to inductive magnets (and vice versa) is known as Curie temperature. Although the torques in each particle are in the same direction, the magnetic moment of the system consists of pure magnetic nanoparticles equal to zero. After being placed in the magnetic field, the torques are aligned and obtain magnetism [5-7]. Cisplatin ($\text{Cl}_2\text{H}_6\text{N}_2\text{Pt}$), also referred to as cis-diamminedichloroplatinum (II), is a chemotherapy drug used to treat types of cancer such as testicular, ovarian, cervical, breast, and bladder cancer [8-10]. Cisplatin is delivered intravenously as a short-term treatment with malignant saline [11]. Cisplatin induces apoptosis by interfering with the mitotic cell division process in tumor cells, which may cause neurological complications. Recent studies have shown that noncompetitive cisplatin inhibits the transport of hydrogen sodium, acting as a membrane inhibitor.

Cisplatin binds to DNA in various ways and interferes with mitosis and DNA repair, activating apoptosis. In 2008, researchers showed that cisplatin-induced apoptosis was dependent on mitochondrial human cancer cells. Thus, cisplatin-induced apoptosis may also be involved in other tissues [12, 13]. Cisplatin is widely used as a potent antitumor treatment. In the treatment of solid tumors, it interferes with the transcriptional process of the tumor cells while not harming the healthy cells because they are chemically degradable,

less soluble in water, and have low cholesterol properties. Cisplatin drugs, combined with magnetic nanoparticles, are developed as hydrophilic polymers. Their structure and chemical properties are protected by the magnetic core and the polymeric shell, which decomposes due to pH conditions and enzymes in the target tissue, and its therapeutic properties apply. It is then absorbed into the reticuloendothelial system and cleansed in the bloodstream. Porous magnetic nanoparticles are also used as magnetic shells containing cisplatin drug nuclei. They are crystalline with pores of about 3 nm, which are stable under physiological conditions. Porous magnetic nanoparticles, in combination with immunoglobulins, can deliver cisplatin to breast cancer tumor tissue. The carboxylic and amine groups of the magnetic Nano clay coating polymers increase the release of cisplatin into the target tissue. After being released into the cytoplasmic lysosomes, cisplatin breaks down into the lysosomes in acidic conditions, penetrates into the nucleus through intracellular endocytosis, and decomposes into the target cell nucleus [14-17].

In 2004, Gupta *et al.* [18] conducted a study on the synthesis of superoxide nanoparticles and modification of their surface with polyethylene glycol polymer for drug delivery using paclitaxel anticancer drug. Using the inverse microemulsion polymerization process, they were able to synthesize magnetic polymeric nanoparticles consisting of a magnetic core and a polymeric shell. Physical and chemical studies such as TEM and AFM have shown that the nanoparticles coated with polyethylene glycol have a spherical shell-core structure. In this study, the cytotoxicity of the synthesized nanoparticles was evaluated using the MTT test on human skin fibroblast cells. It was observed that magnetic nanoparticles modified by polyethylene glycol are non-toxic.

MTT test results showed that the viability of cells treated with polyethylene glycol-modified nanoparticles for 24 h increased by 10 to 40% compared to untreated control samples. The overall result was that polyethylene glycol-modified nanoparticles are suitable for biomedical applications in both in vitro and in vivo conditions.

In 2010, they conducted a study on the synthesis of iron oxide nanoparticles and modification of their surface with Tween 80 and its cellular side by MTT assay. This study aimed to investigate the concentration on the cytotoxic potential of nanoparticles, the influence of time parameters, and the induction of oxidative stress by iron oxide nanoparticles. The results revealed that most cells were killed during the apoptosis process. Production of reactive oxygen species increased by higher concentrations of nanoparticles, leading to cell damage and death [19].

In 2010, Kajal *et al.* [20] synthesized iron oxide nanoparticles for magnetic targeting of drugs to treat cancer areas. They synthesized the nanoparticles by co-precipitating iron oxides and modified their surface with polyvinyl alcohol. After loading the drug and conducting the necessary studies, it was concluded that the polyvinyl-alcohol-modified nanoparticles have a high potential for magnetic targeting of the drug.

In 2010, a study was conducted on synthesizing iron oxide nanoparticles for the magnetic targeting of drugs and for the treatment of cancer areas. They synthesized iron oxide nanoparticles by co-precipitation method and modified their surface with polyvinyl alcohol. After loading the drug and necessary investigations, it was inferred that nanoparticles modified with polyvinyl alcohol have a high potential for magnetic targeting of the drug [21].

In 2012, they investigated the effect of encapsulated cisplatin in nano-containing archaeosomes on the growth of breast cancer cells in gut cellule MCF-7, and the results showed that the efficacy of encapsulated cisplatin is greater than the free drug [22]. The cytotoxicity of cisplatin in ovarian cancer cells was investigated. Results showed that cisplatin had a positive effect on cancer cells and suggested the possibility of using this drug to prevent the implantation of tumor cells [23]. In 2015, the biological properties of Herceptin in cancer cells were studied, and findings indicated that Herceptin could be a promising candidate in cancer diagnostic applications [24]. In 2013, Mokhtari *et al.* investigated the effect of cisplatin and cisplatin loaded on magnetic iron oxide nanoparticles on T47D class of breast cancer cells; findings showed that loaded cisplatin was more likely to kill cancer cells than free cisplatin [25].

This study aimed to synthesize cisplatin magnetic nanocomposites with the possibility of being targeted to cancer cells.

Experiments

Materials and Methods

The chemicals used in this study were from Merck, including iron chloride (III), iron chloride (II), ammonium hydroxide (25%), ethanol, sodium hydroxide, 3-aminopropyl trimethoxysilane (APTMS), ethyl alcohol, HCl and cisplatin. Deionized water was used throughout the experiments.

Synthesis of Superparamagnetic Magnetic Nanoparticles

Wet co-precipitating method was used to synthesize nanomagnetites. Initially, we poured 1.59 g of $\text{FeCl}_2 \cdot 4\text{H}_2\text{O}$ and 3.33 g of $\text{FeCl}_3 \cdot 6\text{H}_2\text{O}$ into a double-opening balloon and placed a

magnet into it using 100 mL of deionized water resolved (It had been under nitrogen gas for about half an hour). The solution turned yellowish-orange. The solution was stirred under N₂ gas for 10 min at 80 °C. Then, 60 mL of 3 M NaOH was immediately poured into the mixture, and the mixture color turned black. The solution was stirred for one hour under N₂ gas. And then, the magnet came out of the solution using magnets. Eventually, the balloon was placed on a strong magnet, and the dissolved precipitate settled. The water above the black precipitate was drained, washed three times with deionized water, and finally dried at room temperature.

Modifying the Surface of Magnetite Nanoparticles with 3-amino Propyl Trimethoxysilane

As much as 6 g of magnetite nanoparticles were dissolved in 150 mL (1-1) water-ethanol solution for 30 min in an ultrasonic dispenser to distribute evenly. The solution was then placed on the heater. Then, 12 mL of 3-aminopropyl trimethoxysilane (APTMS) was added to it, being refluxed for two hours at 40 °C under N₂ gas. After two hours, we put the reflux magnet under the human overflow of the precipitate and washed the precipitate with distilled water and ethanol, which was then dried at room temperature [26].

Loading of cisplatin into a magnetic nanocomposite modified with 3-aminopropyl trimethoxysilane

As much as 0.1 g of the nanoparticles in step 2 was dispersed in 10 mL of ethyl alcohol and 25 mL of ammonia. In another container, 0.1 mL of cisplatin was dissolved in 25 mL of 0.2 M HCl and heated in a warm bath at 80 °C for several

hours. The solution was then added to a container of Fe₃O₄-APTMS and separated for 24 h by stirring after a magnetic reaction with Fe₃O₄-APTMS-cisplatin. It is washed three times with deionized water then dried in a vacuum at 85 °C for 3 h.

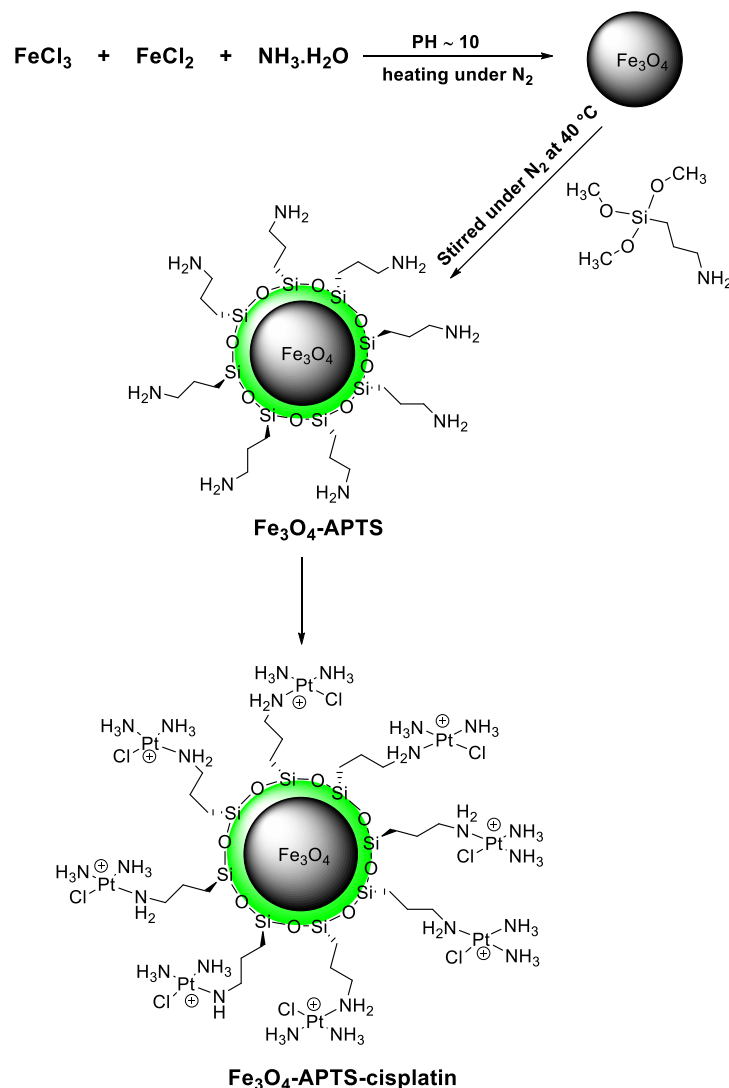
Instrumentation

The powder XRD was performed at room temperature with a PW 1800 (PHILIPS) X-ray diffractometer equipped with a Cu-K α radiation source ($k = 0.154056$ nm). The positions and full width determined the lattice constant and the average crystallite size at half maximum (FWHM) of the (311) peaks by using the Scherrer formula. Element analysis was carried out by an energy dispersive X-ray analysis (EDAX) on a field emission scanning electron microscopy (FESEM, Hitachi F4160 oxford instrument). The morphology of the particles was observed by a transmission electron microscope (TEM) (JEM2010). For characterizing the likely impure phase of the residual organic materials that XRD cannot detect, the Fourier transform infrared spectra (FT-IR) (NICOLET 5700) were also measured. Magnetic measurements were performed using a vibrating sample magnetometer (VSM) on a physical property measure system (VSM Lecshore).

Results and Discussion

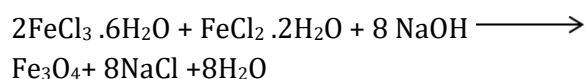
Scheme 1 shows the synthesis plan of nano-magnetite modified with 3-amino propyl trimethoxysilane and the loading of cisplatin on it, which was investigated and identified by various analyzes.

The following mechanism tells how the desired products are formed at each step (Scheme 1):



Scheme 1. Synthesis plan and surface modification of magnetic nanocomposites with cisplatin

Co-precipitating method was adopted to form magnetite nanoparticles (Fe_3O_4). In this method, magnetite nanoparticles were obtained by precipitating iron (II) and iron (III) salts with a stoichiometric ratio of 1: 2 in the basic solution.



3-Aminopropyl trimethoxysilane was used to place the amino group on the surface of the magnetite nanoparticles. During this reaction, methoxy groups of the reactant were removed,

and the resulting Si-O-Si bonds caused the aminopropyl group to bind to the surface of the magnetite nanoparticles.

Cisplatin can attach to the surface of the nanoparticles and then is detached in acidic milieu media by pH-dependent interactions between cisplatin and the nanoparticle. In this mechanism, the bond between chlorine and platinum is broken down in an acidic environment, and released NH_2 from amino-modified nanoparticles binds to platinum.

Investigation of FT-IR spectrum of magnetite nanoparticles and modified magnetite nanoparticles with 3-amino propyl trimethoxysilane attached to cisplatin

Figure 1(a) reveals the FT-IR spectrum related to obtained magnetite nanoparticles. Peaks related to Fe-O bonding are seen at 448cm^{-1} and Fe-O bonding at 565cm^{-1} . The peaks at 3393cm^{-1} and 1625cm^{-1} are related to the tensile and flexural vibrations of the surface of hydroxyl groups, respectively.

Figure 1(b) shows the FT-IR spectrum of the resultant compound. The silica network is deposited on the surface of the nanoparticles by Fe-O-Si bonds. The peaks at 1084cm^{-1} indicate

Si-O-Si bonds. The wide peak at 3413cm^{-1} and the partly sharp peak at 1632cm^{-1} are related to the tensile and flexural vibration of the NH bond, respectively. The peaks at 465 and 568cm^{-1} are also related to Fe-O bonds in magnetite nanoparticles, respectively.

Figure 1(c) shows the FT-IR spectrum of cisplatin-modified nanoparticles. All peaks related to modified magnetite nanoparticles were observed. The peak related to platinum-nitrogen bonding falls below 400 . Only the existence of this linkage is confirmed by EDAX analysis. As previously reported, the particles become less polar as many platinum-bound chlorines could be substituted by the terminal amine group of APTS [27].

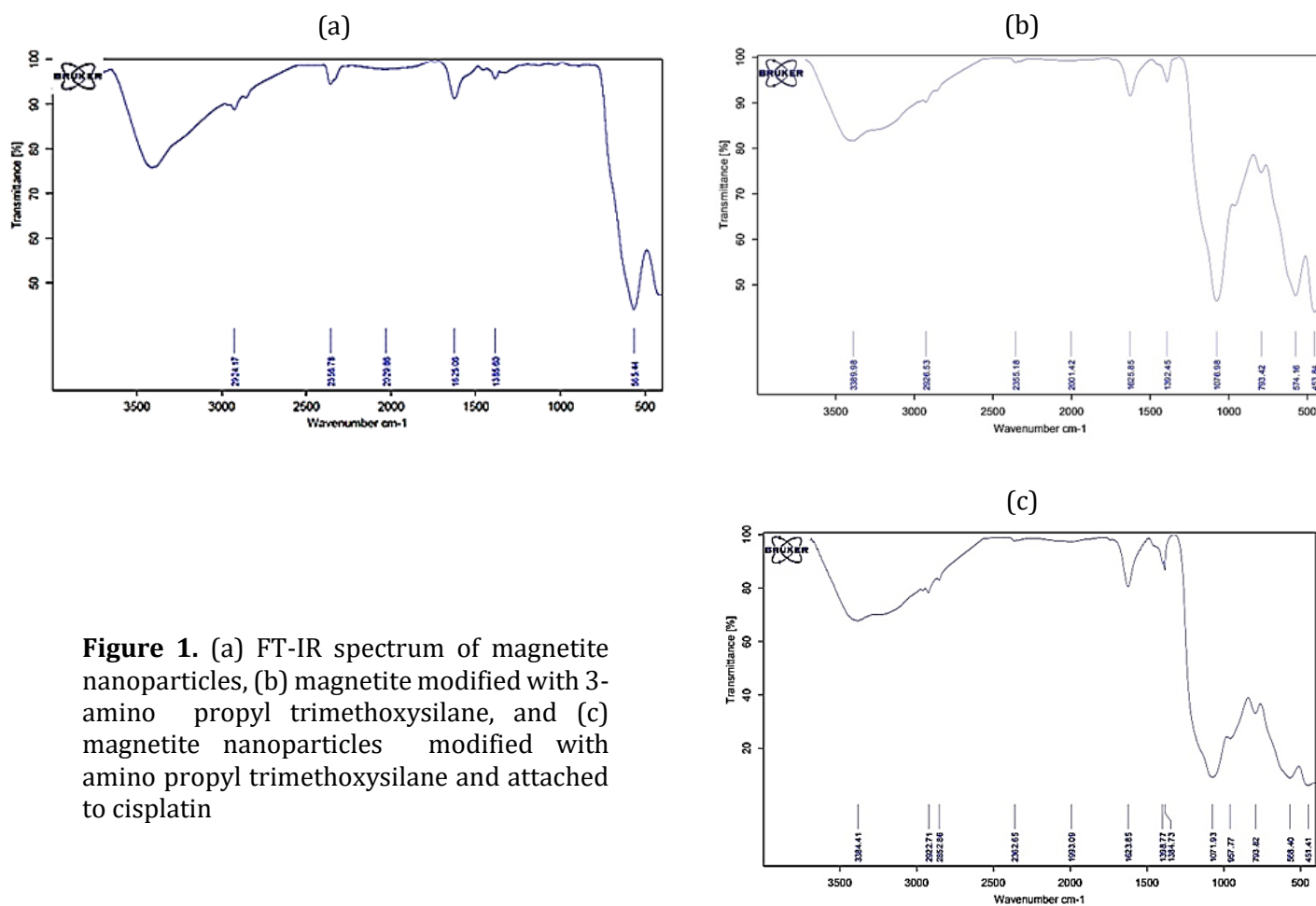


Figure 1. (a) FT-IR spectrum of magnetite nanoparticles, (b) magnetite modified with 3-amino propyl trimethoxysilane, and (c) magnetite nanoparticles modified with amino propyl trimethoxysilane and attached to cisplatin

Investigation of XRD patterns of magnetite nanoparticles and modified magnetite nanoparticles with 3-amino propyl triethoxysilane

Figure 2(a) shows the X-ray diffraction (XRD) pattern of the obtained magnetic nanoparticles. The peaks observed in these patterns have been assigned to the scattering from (220), (311), (400), (422), (511), and (440) planes, all consistent with those of standard XRD pattern of spinel, Fe_3O_4 (JCPDS card No. 86-2267) and confirm maintaining ferrite spinel structure in both cases.

The average crystalline size of nanoparticles at the characteristic peak (311) was calculated

using Scherrer's formula. The average size of the nanoparticles is 8.45 nm.

Figure 2(b) shows the X-ray diffraction pattern (XRD) related to obtained magnetic nanoparticles modified with 3-amino propyl trimethoxy saline. All visible peaks in these patterns correspond to reported data from standard XRD pattern (JCPDS card No. 86-2267) and confirm the nanoparticle crystallinity, and show that surface modification does not change the structure of nano-magnetite. Nanoparticle crystallinity in XRD was calculated by the Debye-Scherrer formula using the highest peak width (311) at half height. The average size of the nanoparticles is 8.43 nm.

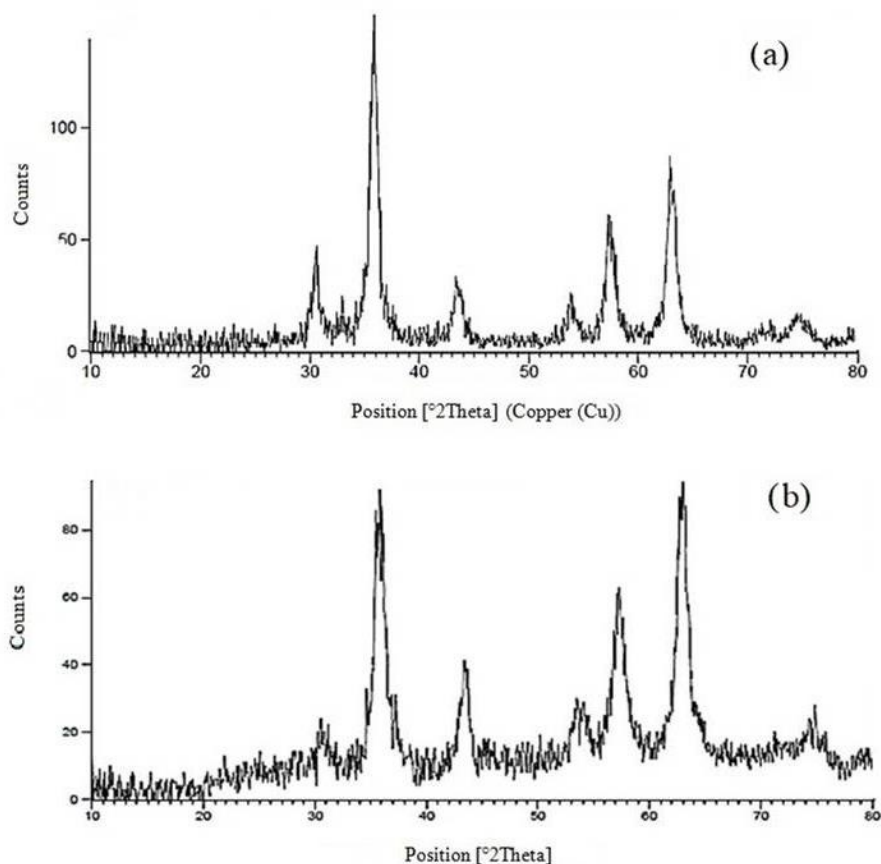


Figure 2. (a) XRD pattern related to magnetite nanoparticles (b) and magnetite nanoparticles modified with amino propyl trimethoxysilane

Magnetic properties of magnetite nanoparticles and magnetite nanoparticles modified with 3-amino propyltrimethoxysilane

VSM analysis was performed to identify the resulting compound, and the field-based magnetization is shown in [Figure 3\(a\)](#). A single-sphere magnetic material, which does not show any residual, rings in its magnetization curve. Therefore, it is indicative of its superparamagnetism. The saturation magnetization of this compound is about 40 emu/g. The field-based magnetization curve for magnetite-modified nanoparticles with 3-amino propyl trimethoxysilane is shown in

[Figure 3\(b\)](#). A single-sphere magnetic material, which does not show any residuals, rings in its magnetization curve, demonstrating its superparamagnetism.

The saturation magnetization of this compound is about 29 emu/g. An exciting new change in the hysteresis loop is observed for modified nanoparticles. A magnetic saturation reduced to $M_s=29\text{emu/g}$ and close to zero for coercivity and remanence shows a superparamagnetic behavior. Lower magnetic saturation, in this case can be related to the separation of neighboring nanoparticles by a silica layer leading to a weaker magnetostatic coupling between the particles ([Table 1](#)).

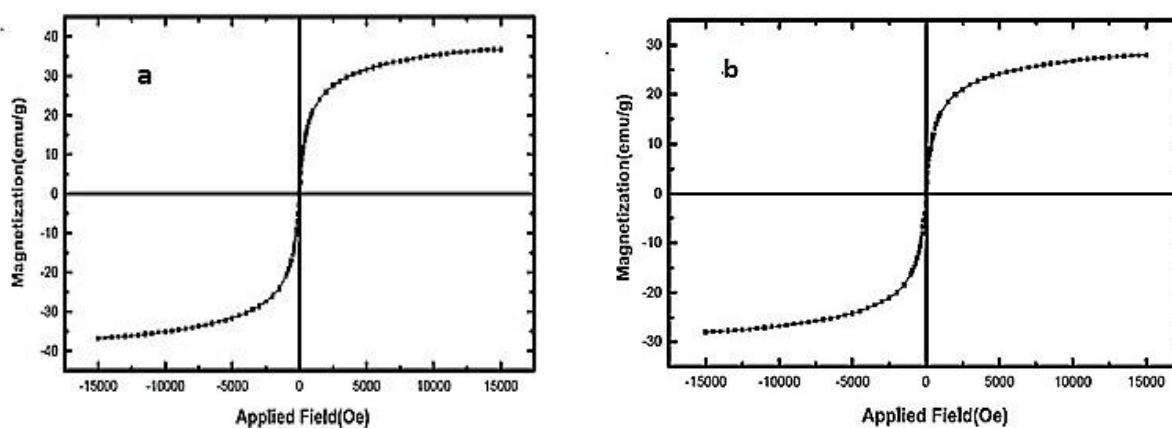


Figure 3. (a) Hysteresis loops of the as-prepared Fe_3O_4 nanoparticles with a magnetic field of 15kOe (b) magnetite nanoparticles modified with aminopropyltrimethoxysilane

Table 1. Comparison of the magnetic parameters of the synthesized nanoparticles

Samples	M_s (emu/g)	H_c (Oe)
Fe_3O_4	40 emu/g	0
$\text{Fe}_3\text{O}_4\text{@APTMS}$	29 emu/g	0

Investigation of SEM and EDAX images related to magnetite nanoparticles and magnetite nanoparticles modified with 3-amino propyl trimethoxysilane attached to cisplatin

[Figures 4\(a\)](#) and [5\(a\)](#) demonstrate SEM and EDAX images related to magnetite

nanoparticles with a magnification of 200 nm, respectively. These images show good homogeneous distribution of spherical nanoparticles. The EDAX spectrum shows the presence of Fe and O in the composition.

Figures 4(b) and 5(b) show the SEM and EDAX images related to the magnetite nanoparticles modified with 3-amino propyltrimethoxysilane, respectively, showing

good homogeneous distribution of spherical nanoparticles. EDAX spectrum shows the presence of C, N, and Si in addition to Fe and O in the composition.

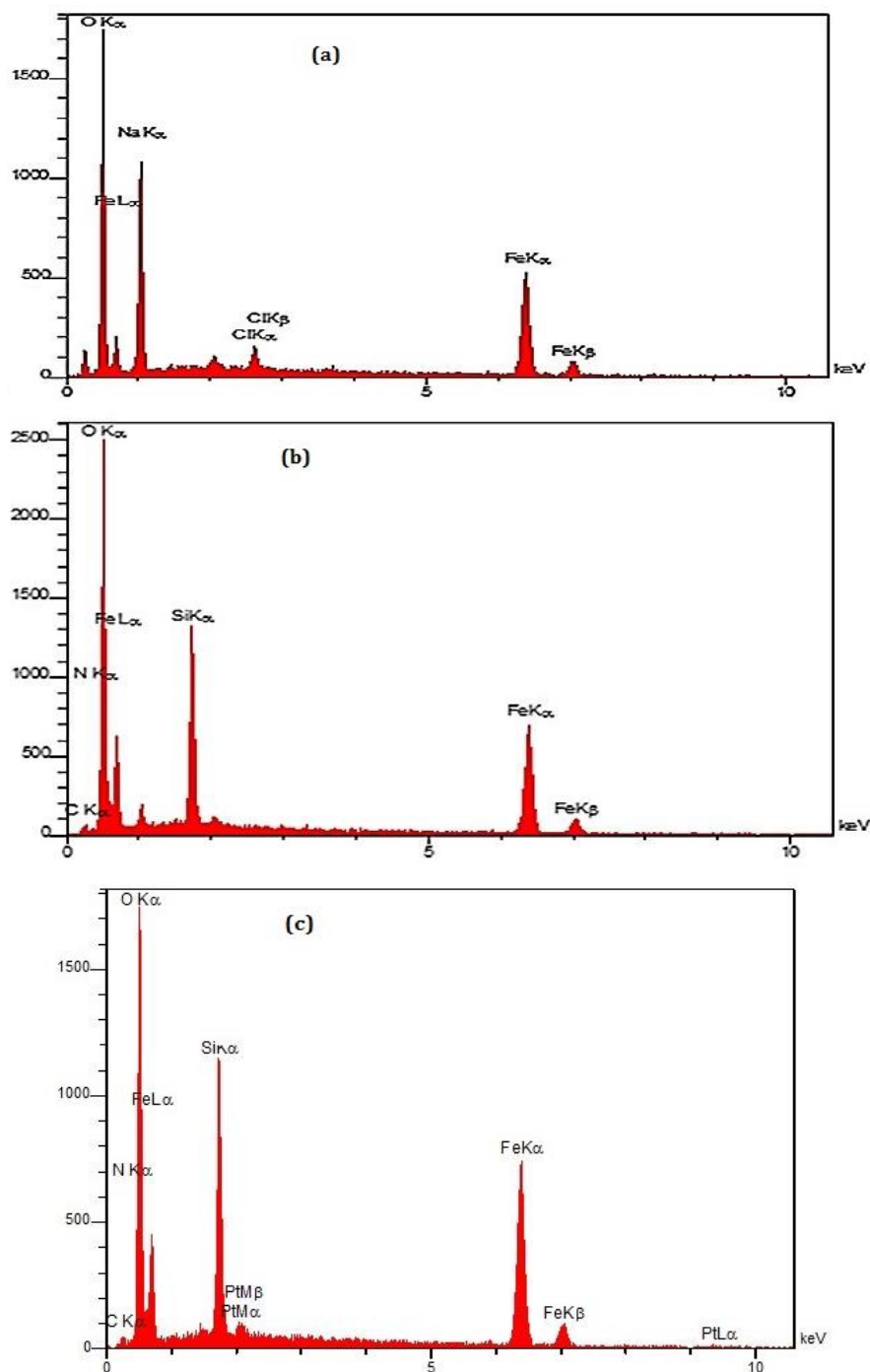


Figure 4. (a) EDAX images of magnetized magnetite nanoparticles with magnification of 200 nm (b) of Magnetite modified with 3-amino propyl trimethoxysilane nanoparticles (c) of magnetite nanoparticles modified with 3-amino propyl trimethoxysilane attached to cisplatin

Figures 4(c) and 5(c) depict the SEM and EDAX images of the magnetite nanoparticles modified with 3-amino propyltrimethoxysilane attached to cisplatin at 200 nm, respectively. These

images show good homogeneous distribution of spherical nanoparticles. The EDAX spectrum shows the presence of Pt in addition to Fe, O, Si, N, and C (Table 2).

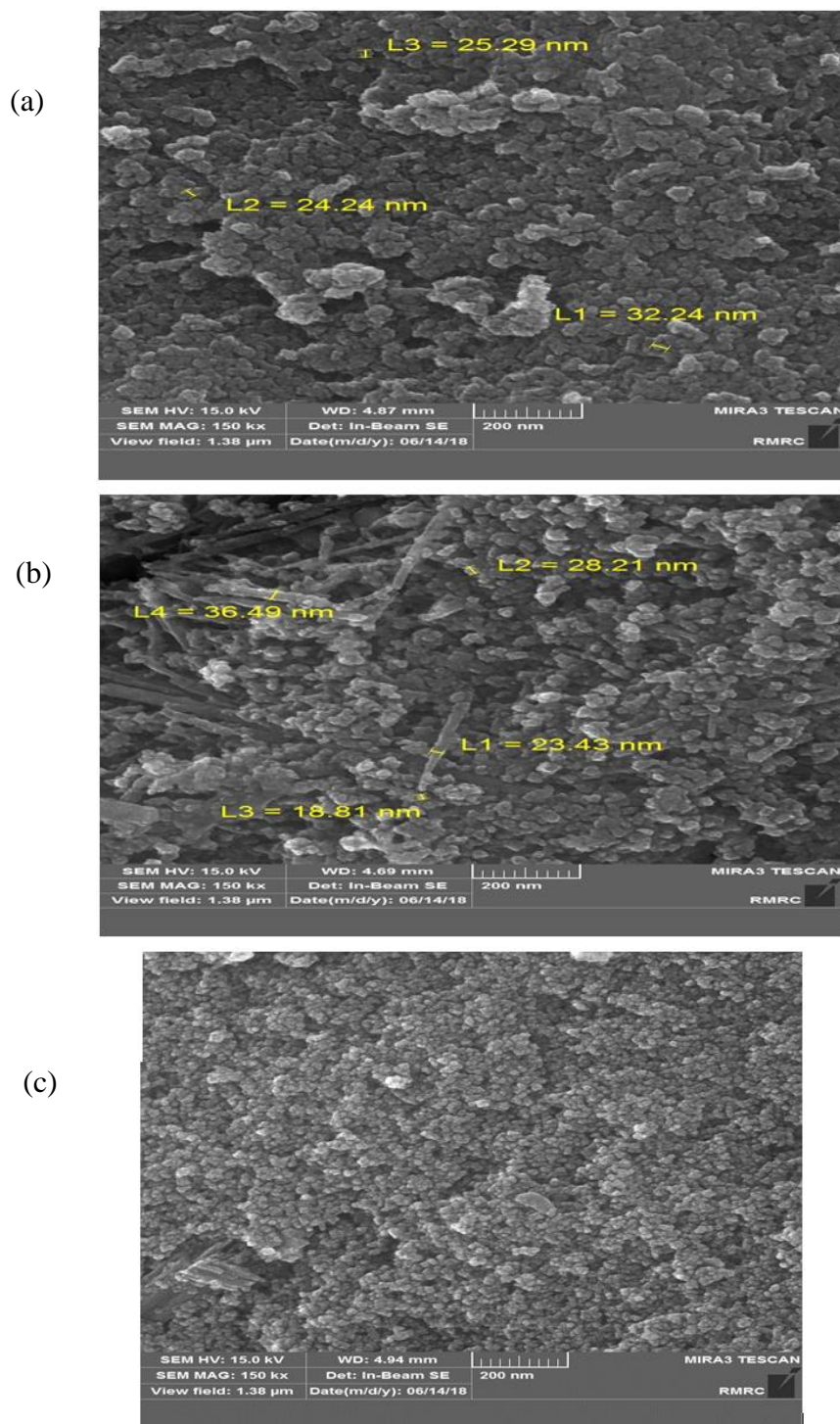


Figure 5. (a) SEM images of magnetized magnetite nano-particles with the magnification of 200 nm; (b) magnetite modified with 3-amino propyl trimethoxy-silane; and (c) magnetite modified with 3-amino propyl trimethoxy-silane attached to cisplatin

Table 2. EDAX quantification (standard less) element normalized for magnetite nanoparticles modified with 3-amino propyl trimethoxysilane attached to cisplatin

Quantitative results											
Elt	Line	Int	Error	K	K _r	W%	A%	ZAF	Formula	O _x %	P _k /Bg
C	K _a	9.5	2.7926	0.0156	0.0106	4.13	8.42	0.2571	-	0.00	5.77
N	K _a	2.7	2.7926	0.0061	0.0041	1.08	1.89	0.3823	-	0.00	2.48
O	K _a	421.4	2.7926	0.3445	0.2346	42.17	64.55	0.5564	-	0.00	35.88
Si	K _a	318.3	0.9895	0.0954	0.0650	8.89	7.75	0.7310g	-	0.00	18.21
Fe	K _a	344.4	0.7388	0.4893	0.3332	38.06	16.69	0.8757	-	0.00	38.15
Pt	L _a	2.0	0.4058	0.0491	0.0335	5.68	0.71	0.5897	-	0.00	2.34
				1.0000	0.6810	100.00	100.00		-	0.00	

Investigation of TEM image related to magnetite nanoparticles modified with 3-amino propyl trimethoxysilane attached to cisplatin

Figure 6 reveals the TEM image of Fe₃O₄-APTMS-cisplatin. The morphologies showed a spherical shape with the homogeneous

dispersed distribution. The average sizes of the nanoparticles are close to the crystalline grain values calculated using Scherrer's equation. The slight difference may be due to the presence of multi-grain particles. It is observed that the crystallite size of Fe₃O₄-APTMS-cisplatin is estimated to be in the range of 15-30 nm.

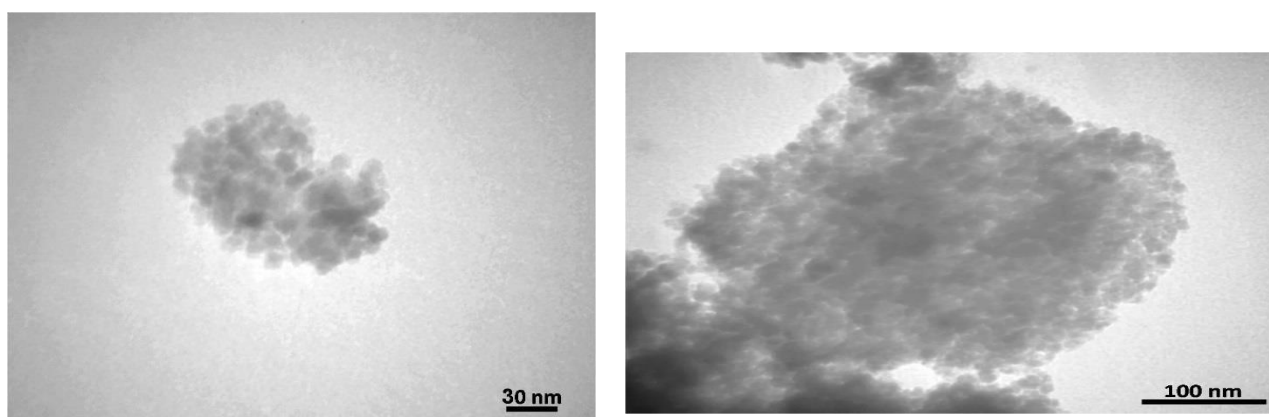


Figure 6. TEM images of the Fe₃O₄-APTMS-cisplatin Nanocomposite

Conclusion

The problem with the treatment of many types of cancer is the lack of specific drug delivery to the surface of and inside the cancer cells, which can damage healthy cells, bringing about side effects and even death for patients who undergo chemotherapy. The purpose of a stabilized drug in magnetic materials under an external magnetic field.

In this study, cisplatin magnetic nanocomposite, was prepared by co-precipitation method and identified by (FT-IR),(XRD), (SEM-EDAX), (VSM), and (TEM) techniques. Magnetic measurements of the superparamagnetic properties. The synthesized cisplatin nanoparticles in this study had an average size of 30 nm by binding through an amine agent with equal magnetic properties; it can be used to create magnetic fields toward targeted transfer to cancer cells. SEM and EDAX confirmed the spherical shape of the magnetically synthesized nano-cisplatin. Physical and chemical studies such as TEM have shown that the nanoparticles coated with - amino propyl trimethoxysilane have a shell-core structure and are spherical. A successful synthesis of magneto-cisplatin nano materials and the presence of high magnetic field properties, on the one hand, its spherical shape and the other hand, may justify using this drug as a good candidate in chemotherapy.


Acknowledgments

We are grateful to Islamic Azad University for its financial support.

Disclosure Statement

No potential conflict of interest was reported by the authors.

Orcid

Haniye Pourfaraj : 0009-0000-4664-8177

Somayyeh R. Mansour : 0000-0003-2487-0978

Mohammad Zaefizadeh : 0000-0001-6539-6550

Arash Vojood : 0000-0002-2658-9664

References

- [1]. Faraji M., Yamini Y., Rezaee M. *J. Iran. Chem. Soc.*, 2010, **7**:1 [[CrossRef](#)], [[Google Scholar](#)], [[Publisher](#)]
- [2]. Malhotra N., Lee J.S., Liman R.A.D., Ruallo J.M.S., Villaflores O.B., Ger T.R., Hsiao C.D. *Molecules*, 2020, **25**:3159 [[CrossRef](#)], [[Google Scholar](#)] [[Publisher](#)]
- [3]. Lu A.H., Salabas E.L., Schüth F. *Angew. Chem. Int. Ed.*, 2007, **46**:1222 [[Crossref](#)], [[Google Scholar](#)], [[Publisher](#)]
- [4]. Dehno Khalaji A., Jarosova M., Machek P. *Asian J. Green Chem.*, 2021, **5**:351 [[Crossref](#)], [[Publisher](#)]
- [5]. Reddy L.H., Arias J.L., Nicolas J., Couvreur P. *Chem. Rev.*, 2012, **112**:5818 [[Crossref](#)], [[Google Scholar](#)], [[Publisher](#)]
- [6]. Pourbahar N., Sattari Alamdar S. *Asian J. Green Chem.*, 2023, **7**:9 [[Crossref](#)], [[Publisher](#)]
- [7]. Seifi Mansour S., Ezzatzadeh E., Safarkar R. *Asian J. Green Chem.*, 2019, **3**:351 [[Crossref](#)], [[Publisher](#)]
- [8]. Oun R., Moussa Y.E., Wheate N.J. *Dalton Trans.*, 2018, **47**:6645 [[Crossref](#)], [[Google Scholar](#)], [[Publisher](#)]
- [9]. Forgie B.N., Prakash R., Telleria M. *Int. J. Mol. Sci.*, 2022, **23**:15410 [[Crossref](#)], [[Google Scholar](#)], [[Publisher](#)]
- [10]. Deljoo S., Rabiee N., Rabiee M. *Asian J. Nanosci. Mater.*, 2019, **2**:66 [[Crossref](#)], [[Google Scholar](#)], [[Publisher](#)]
- [11]. Milosavljevic N., Durantou C., Djerbi N., Puech P.H., Gounon P., Lagadic-Gossmann D., Dimanche-Boitrel M.T., Rauch C., Tauc M.,

- Counillon L. Poët M., *Cancer Res.*, 2010, **70**:7514 [Crossref], [Google Scholar], [Publisher]
- [12]. Pruefer F.G., Lizarraga F., Maldonado V., Melendez-Zajgla J. *J. Chemother.*, 2008, **20**:348 [Crossref], [Google Scholar], [Publisher]
- [13]. Salimi F., Dilmaghani K.A., Alizadeh E., Akbarzadeh A., Davaran S. *Artif. Cells, Nanomed., Biotechnol.*, 2018, **46**:949 [Crossref], [Google Scholar], [Publisher]
- [14]. Cheng K., Peng S., Xu C., Sun S. *J. Am. Chem. Soc.*, 2009, **131**:10637 [Crossref], [Google Scholar], [Publisher]
- [15]. Shakoori Z., Pashaei-Asl R., Pashaiasl M., Davaran S., Ghanbari H., Ebrahimie E., Mahdi S. *J. Drug Delivery Sci. Technol.*, 2022, **71**:103254 [Crossref], [Google Scholar], [Publisher]
- [16]. Brown A., Kumar S., Chounwou P.B. *J. Cancer Sci Ther.* 2019, **11**:97 [Crossref], [Google Scholar], [Publisher]
- [17]. Aldossary S.A. *Biomed. Pharmacol. J.*, 2019, **12**:7 [Google Scholar]
- [18]. Gupta A.K., Wells S. *IEEE transactions on nanobioscience.*, 2004, **3**:66 [Crossref], [Google Scholar], [Publisher]
- [19]. Aljarrah K., Mhaidat N.M., AlAkhras M.A., Aldaher A.N., Albiss B., Aledealat K., Alsheyab F.M. *World J. Surg. Onc.*, 2012, **10**:62 [Crossref], [Google Scholar], [Publisher]
- [20]. Kayal S., Ramanujan R.V. *Mater. Sci. Eng. C.*, 2010, **30**:484 [Crossref], [Google Scholar], [Publisher]
- [21]. Tian X., Wei F., Wang L., Yu W., Zhang N., Zhang X., Han Y., Yu J., Ren X. *Front. Immunol.*, 2017, **8**:1426 [Crossref], [Google Scholar], [Publisher]
- [22]. Kim J.E., Young S.H., Cho M.H. *Arch. Toxicol.*, 2012, **86**:685 [Crossref], [Google Scholar], [Publisher]
- [23]. Fanning J., Biddle W.C., Goldrosen M., Crickard K., Crickard U., Piver M.S., Foon K.A. *Gynecol. Oncol.*, 1990, **39**:119 [Crossref], [Google Scholar], [Publisher]
- [24]. Salunkhe A.B., Khot V.M., Thorat N.D., Phadatare M.R., Sathish C.I., Dhawale D.S., Pawar S.H. *Appl. Surf. Sci.*, 2013, **264**:598 [Crossref], [Google Scholar], [Publisher]
- [25]. Mokhtari M., Hoseinian Z.H., Koohepyma F., Akbarzadeh A., Hashemi M.M., Kamyab A., Mohammadi H. *Pathobiol. Res.*, 2013, **15**:75 [Google Scholar], [Publisher]
- [26]. Palimi M.J., Rostami M., Mahdavian M., Ramezanzadeh B. *Appl. Surf. Sci.*, 2014, **320**:60 [Crossref], [Google Scholar], [Publisher]
- [27]. Bhowmick T., Yoon D., Patel M., J. Fisher, Ehrman S. *J. Nanopart. Res.*, 2010, **12**:2757 [Crossref], [Google Scholar], [Publisher]

How to cite this manuscript: H. Pourfaraj, S. Rostamzadeh Mansour*, M. Zaefizadeh, A. Vojood. Synthesis and Characterization of Cisplatin Magnetic Nanocomposite. *Journal of Medicinal and Nanomaterials Chemistry*, 5(1) 2023, 92-105. DOI: [10.48309/JMNC.2023.1.6](https://doi.org/10.48309/JMNC.2023.1.6)